The Sixth Asia-Pacific Conference on
Wind Engineering(APCWE-VI)
Seoul, Korea, September 12-14, 2005

A Field Test and Full Dynamic Simulation on a Stall Regulated Wind Turbine

Takeshi Ishihara[1)], Pham Van Phuc[2)], Yozo Fujino[2)], Keiji Takahara[3)]
and Takehiro Mekaru[3)]

[1)] *Institute of Eng., Innovation School of Eng., The University of Tokyo, 2-11-16, Japan*
[2)] *Department of Civil Engineering, The University of Tokyo, 2-11-16, Japan*
[3)] *Research and Development Dept., The Okinawa Electric Power Co., 5-2-1, Japan*
[1)] *ishihara@bridge.t.u-tokyo.ac.jp*

ABSTRACT

A field test on a stall regulated wind turbine with a rated power of 400 kW at Karimata, Miyakojima Island was carried out to investigate structural parameters as well as wind loads and responses of the turbine. The observed acceleration responses of the tower were used to estimate the natural frequencies and damping ratios of the turbine. The lower natural frequencies of wind turbine such as 0.81Hz and 2.43Hz coincided with the first natural frequencies of the tower and blades. The damping ratios of the tower were around 1% in the fore-aft direction and 0.6% in the side-side direction, respectively. The strains obtained at the root of the tower were used to estimate the tower bending moments. A FEM code was developed to predict natural frequencies and wind loads on the turbine. The observed natural frequencies of the wind turbine were predicted successfully using a full wind turbine model, while a tower model, in which the blades, hub and nacelle were modeled by a concentrated mass at the top of tower, presents the first natural frequency of the tower with 5% of error. The maximum, the mean and the standard deviation of tower bending moments predicted by the full dynamic simulation show a good agreement with the measurements.

INTRODUCTION

Damages of wind turbines located on Miyakojima Island by Typhoon Maemi in 2003, reported by Ishihara et al. (2005), are serious problem in Japan. It is strongly required to investigate the reason of the damages.

---
1) Associate Professor
2) Graduate Student and Professor
3) Researcher

Fig.1 shows three NEG Micon wind turbines with a rated power of 400kW located at Karimata, northern end of Miyakojima Island, two of them were collapsed due to the buckling of the towers near the entrance door and the other was survived. To estimate the wind loads on the turbines during Typhoon Maemi, the structural properties such as geometry, materials, stiffnesses as well as damping ratios of the tower and blades were needed. Since the structural properties were not supplied sufficiently by the manufacturer, onsite investigations were carried out and wind turbine models were constructed, which were used to estimate the maximum wind loads on the tower and blades.

In this study, a field test was carried out to obtain acceleration responses of the tower for the survived turbine to evaluate the natural frequencies and the damping ratios of the turbine. Strains at the root of tower were also observed to estimate the tower bending moments. A FEM code was developed to predict natural frequencies and wind loads on a turbine.

This paper began with the introduction of the field measurements, discussed field test results including wind direction and wind speed at the site, acceleration responses of the tower, strains at the root of tower, and estimated natural frequencies, damping ratios and the wind loads. The natural frequencies of the tower model and the full wind turbine model with beam elements was calculated and compared with observed natural frequencies of the turbine to investigate the reliability of structural parameters such as damping ratios, aerodynamic coefficients used in the simulations. Finally, a full dynamic simulation was carried out and the results were compared with measurements to verify the FEM code developed in this study.

Fig. 1 Damaged wind turbines on Miyakojima Island during Typhoon Maemi in 2003

MESURMENT SYSTEM

In this study, a field test was designed for the survived wind turbine and main characteristics of the wind turbine are shown in Table 1. This stall regulated wind turbine was installed in 1995. The rotor diameter and hub height are 31m and 36m, respectively. The field measurement for the characteristics of wind as well as acceleration responses and strains of the tower was carried out from Jan.16th 2004 to Mar.16th 2004. The rotor and yaw angle were fixed during the measurement.

Table 1 Main characteristics of the observed wind turbine

Name	Description
Installation	December, 1995
Manufacturer	NEG-Micon
Rated power	400kW
Regulation	Stall Regulation
Number of blades	3
Rotor diameter	31m
Hub height	36m

Fig. 2 shows measurement instruments such as the anemometer, accelerometers and strain gauges used in the field test. The configuration of the wind turbine, sensor positions and the coordinates are shown in Fig 3. Here, X and Y denote the fore-aft and the side-side direction of wind turbine, respectively. The azimuth angle of rotor was fixed at 21.27deg and the yaw angle at 56.74deg. A three-cup anemometer and wind vane were attached on the top of the nacelle to measure wind speed and direction at the site. Two sets of SABO accelerometers were installed at the top (35.1 m) and at 2/3 of the height of the tower (26.4m) to obtain the acceleration responses of the tower. At each height, two accelerometers were positioned perpendicularly, so that the acceleration in the two directions can be obtained. Four strain gauges were pasted to the surface of the tower (3.65m from ground) to measure the vertical compressions and tensions at the root of the tower.

a) Anemometer and wind vane

b) Accelerometers

c) Strain gauges

Fig. 2 Measurement instruments

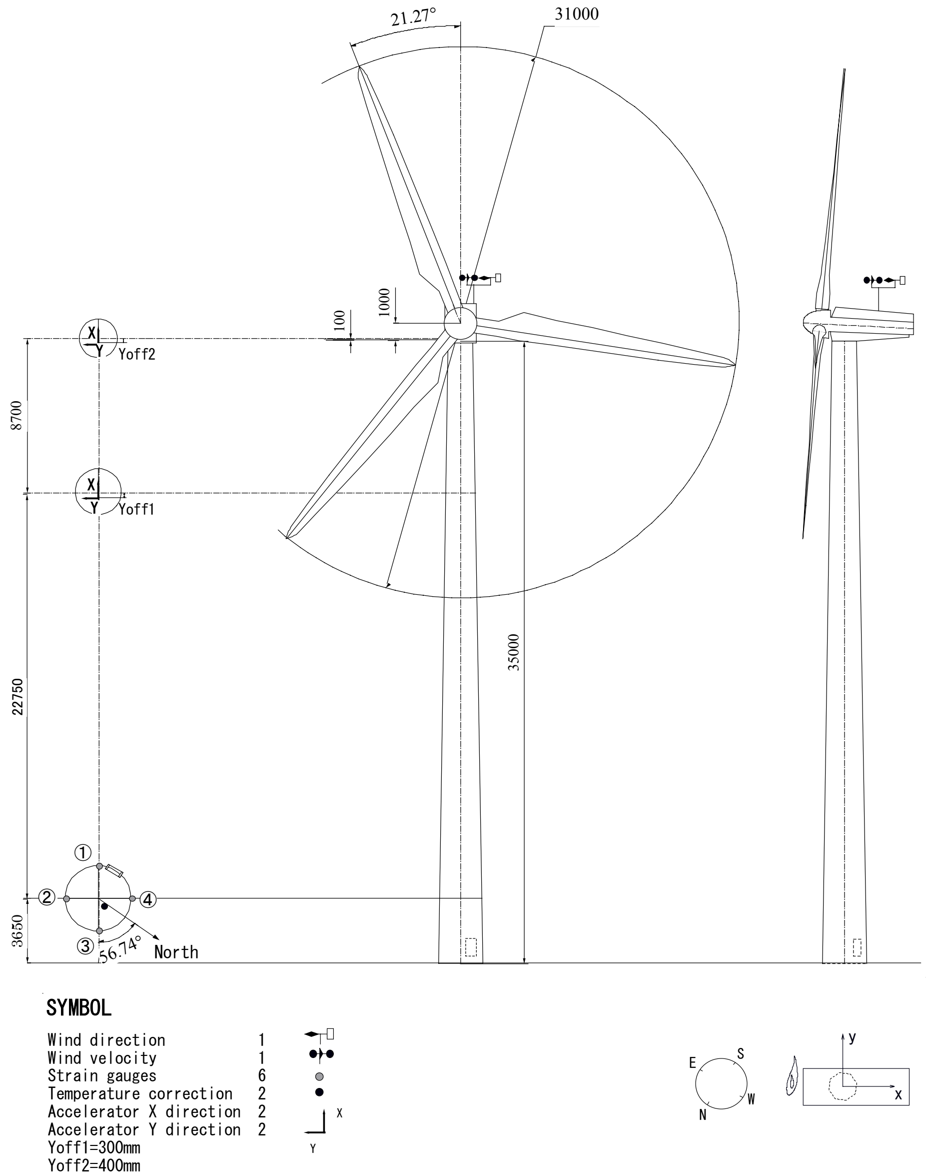

Fig. 3 Configuration of the wind turbine and sensor positions

MESURMENT RESULTS

<u>Characteristics of the wind speed at the site</u>

<u>Maximum wind speeds</u> The wind records were divided into 16 sectors by wind direction. Since three-cup anemometers usually overestimate wind speed, the observed 10-minute mean wind speeds were multiplied by the correction factor of 0.9, as suggested by Ishihara et al. (2002).

Table 2 shows the maximum 10-minute mean wind speed and frequency of occurrence for each wind direction sector during the two months of the measurements. The prevailing wind directions are North-northeast (20.54%), Northeast (17.87%) and North (14.81%), which corresponds to the wind bowing from the front and the right side of the wind turbine. Because the damages by Typhoon Maemi were caused by the northerly wind (see, Ishihara et al. 2005), the data for northerly wind was mainly analyzed.

Table 2 Maximum of wind speeds in 16 wind direction sectors

Wind direction（deg）	0	22.5	45	67.5	90	112.5	135	157.5
Maximum wind speed (m/s)	21.59	16.72	21.01	15.48	9.22	12.03	11.46	14.76
Frequency of occurrence (%)	14.81	20.54	17.87	10.07	6.57	11.21	4.38	4.26

Wind direction（deg）	180	202.5	225	247.5	270	292.5	315	337.5
Maximum wind speed (m/s)	17.80	10.90	11.25	8.70	8.23	5.86	10.04	17.67
Frequency of occurrence (%)	3.20	1.85	1.15	0.94	0.15	0.16	0.44	2.38

Spectrum of wind speed　The spectra of strong wind speeds in the two periods (2:30~2:40 and 2:40~2:50 of Jan.21st 2004) were calculated by the Maximum Entropy Method (MEM). Fig. 2 shows the comparison between observed spectra and von Karman spectrum, as expressed in Eq.(1)

$$\frac{nS(n)}{\sigma^2} = \frac{4x}{\left(1+70.8x^2\right)^{5/6}}, \quad x = nL_x/U \tag{1}$$

Where $S(n)$ is the power spectrum of wind speed, n is the frequency (Hz), σ is the standard deviation of the fluctuating wind speed, U is the mean wind speed and L_x is the integral length scale. The spectra of wind speeds are in agreement with von Karman spectrum.

The integral length scale L_x at the hub height (36m), which is an important parameter to describe the characteristics of turbulence, was estimated to be 133m and 110m for the two periods, respectively and is consistent with a value of 109m for the subcategory I recommend by Architectural Institute of Japan (1996). This is because that wind turbines locate at seaside as shown in Fig. 1, and the roughness at the site can be classified into the terrain subcategory I.

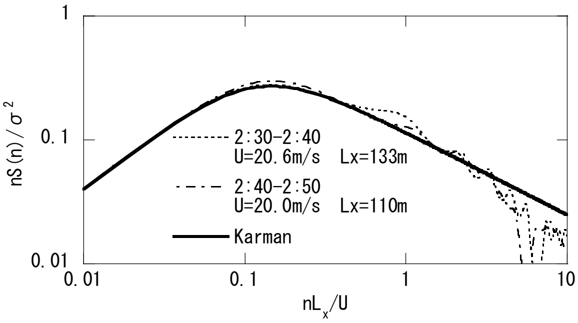

Fig. 2 Comparison of spectra for observed wind speeds and von Karman spectrum.

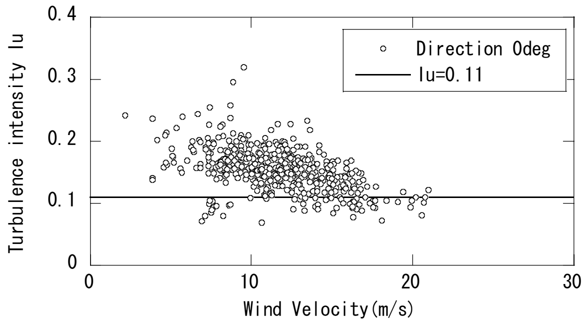

Fig. 3 Variation of turbulence intensities with mean wind speeds

Turbulence intensity The turbulence intensity is defined as the ratio of the standard deviation of fluctuating wind speed to the mean wind speed. Fig. 3 shows the variation of turbulence intensities with mean wind speeds. They decrease and approach to 0.11 when the wind speed increases. It is consistent with the value of 0.13 at the hub height (36m) for the terrain subcategory I, recommended by Architectural Institute of Japan (1996).

Structural dynamic characteristics

Natural frequencies The natural frequencies of the wind turbine are identified from the power spectra of the accelerations as shown in Fig. 4. From the spectra obtained at the top of the tower, the major parts of the energy are found at a natural frequency of 0.81Hz in the X and Y direction. The spectra at the top of the tower also illustrate a significant peak at natural frequency of 2.43Hz, and some peaks at higher natural frequencies such as 4.62Hz and 7.59Hz in X direction. Some other higher natural frequencies, that are 5.6Hz and 6.85Hz in the X direction, as well as 5.6Hz and 6.42Hz in the Y direction, appear obviously at 2/3 of the height of the tower.

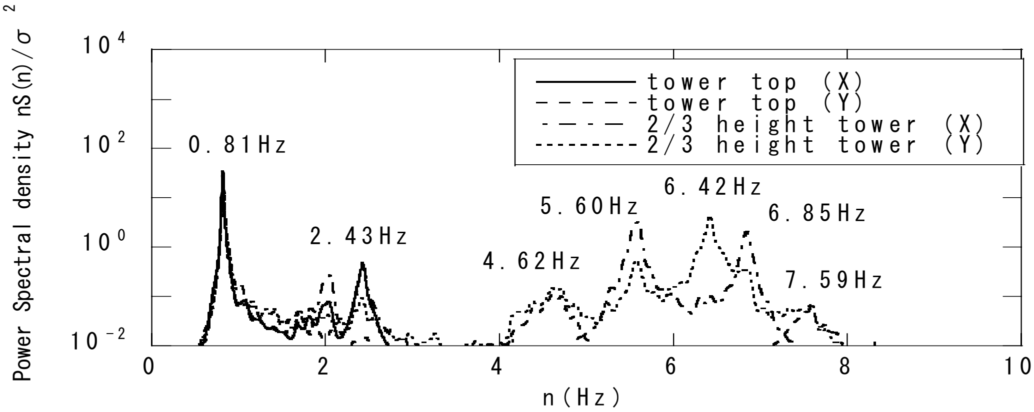

Fig. 4 Power spectral densities of the accelerations at the top and the height of 2/3 of the tower.

<u>Damping ratios</u> The determination of damping ratios is very important to estimate the dynamic responses of structures. Since the Random Decrement Technique (RD technique) is known as an effective method to estimate the damping ratio of structures such as high buildings and towers (Tamura et al.1991), it was used to estimate the damping ratios of the wind turbine in this study.

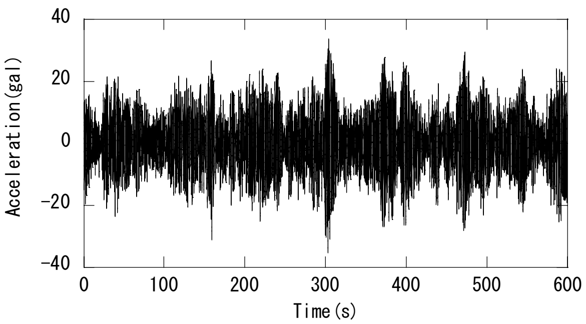

(a) Time series of accelerations

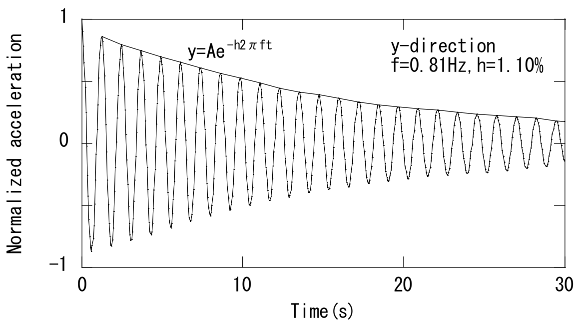

(b) Normalized accelerations

Fig.5 The time series of acceleration response at the top of tower

Fig.5(a) shows an original observed time series of accelerations. The RD technique was applied to remove the random component of accelerations and the normalized acceleration time series is shown in Fig.5 (b). The damping ratios were estimated by using the power exponent function to fit the peaks on the normalized acceleration time series. Fig. 6 presents the variation of damping ratios with the mean wind speed for the first natural frequencies of the tower in the X and the Y direction. The structural damping ratios are around 1% in the X direction, and 0.6% in the Y direction, which are close to empirical value of 0.8% for the tower, as mentioned by Riso National Laboratory (2001).

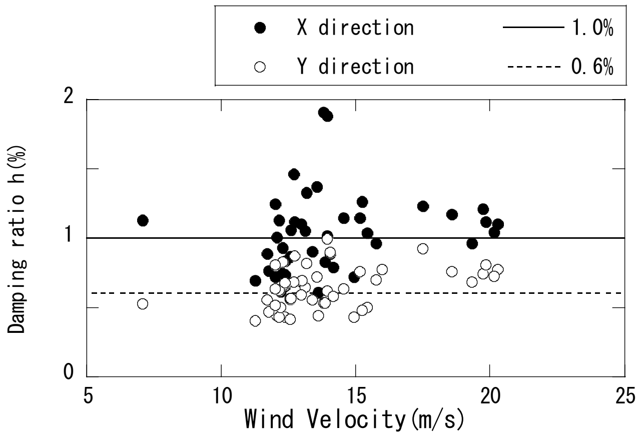

Fig. 6 Variation of the damping ratios with mean wind speeds

Wind loads

The tower bending moments were estimated from the strains obtained at the root of the tower. Fig. 7 gives the definition of the tower bending moments of M_x and M_y, which correspond to the wind loads in the X and the Y direction, respectively. The tower bending moments can be calculated by Eq.(2) and Eq.(3).

$$M_x = EI \times (\varepsilon_3 - \varepsilon_1)/D \quad (2)$$

$$M_y = EI \times (\varepsilon_4 - \varepsilon_2)/D \quad (3)$$

Where E is the Young's modulus, I is the second moment of area, ε_1, ε_4, ε_3 and ε_4 are the strains observed at the positions indicated as ①, ②, ③, ④ in Fig. 3, and D is the tower diameter of the section where the strains were installed.

Fig. 8 shows M_x and M_y plotted in the X-Y plane for the northerly, the easterly and the westerly wind. The tower bending moments draw an elliptical orbit for the northerly wind, and show significant alongwind and acrosswind responses for the easterly and the westerly wind due to a full drag and a full lift acting on the blades, respectively.

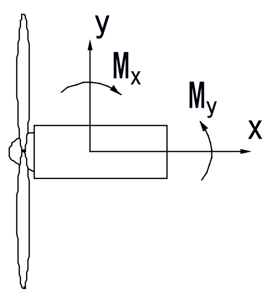

Fig. 7 Coordinate system for the tower bending moments

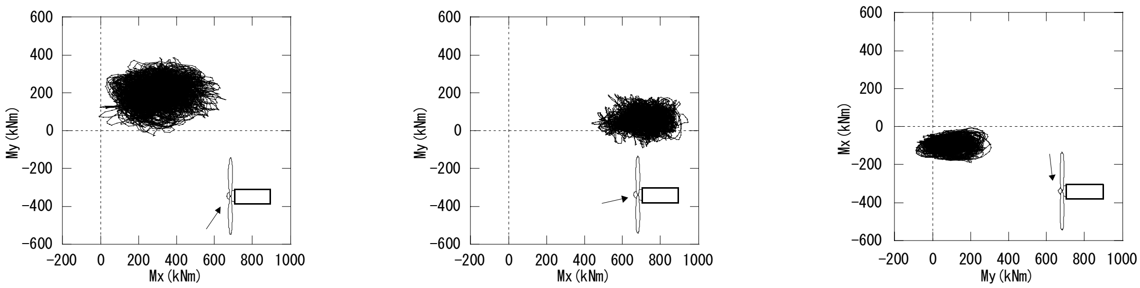

(a) Northerly wind (b) Easterly wind (c) Westerly wind

Fig. 8 Tower bending moments plotted in the X-Y plane.

FULL DYNAMIC SIMULATION

A FEM Code for the full dynamic simulation

In this study, a FEM code called CAsT (Computer-Aided Aerodynamic and Aeroelastic Technology) was developed to predict wind loads acting on wind turbines. A brief description of the CAsT is summarized in Table 3. The beam elements were used for the discretization and the mass of each element was concentrated at its nodes constructing a symmetrical lumped mass matrix. The quasi-steady aerodynamic theory was used to calculate the aerodynamic forces as an external force, in which the drag, the lift force and the moment are estimated by using aerodynamic coefficients and the relative wind velocity. The aerodynamic damping is automatically taken into account during the simulation.

Table 3 A brief description of the FEM code of CAsT

Dynamic analysis	Direct numerical integration, the Newmark method
Eigenvalue analysis	Subspace iteration procedure
Element type	Beam element
Formulation	Total Lagrangian formulation
Aerodynamic force	Quasi-steady aerodynamic theory
Damping	Rayleigh damping

Prediction of natural frequencies

A full wind turbine model with the beam elements was constructed using the structural properties such geometry, material, stiffnesses of the tower and blades obtained from the onsite investigations, and a simplified tower model in which blades, hub and nacelle were approximated by a concentrated mass at the top of the tower was used for comparison. The tower model is known as a model used to predict the modes of tower when the structural properties of the blades are not available.

Table 4 presents the natural frequencies of wind turbine obtained from the field test and those form the analysis using the full wind turbine model and the tower model. The frequencies of 0.85Hz and 6.94Hz obtained from the tower model, corresponding to the first and the second natural frequencies of the tower in X and Y direction, are slightly higher than those obtained from the observation, while the frequencies obtained from the full wind turbine model show a good agreement with the natural frequencies of 0.81Hz from the observation. A blade model with beam elements was also constructed in order to investigate the modes with the higher natural frequencies obtained from the measurement. The frequencies of 2.58Hz from the blade model as shown in Table 5 coincide with the frequencies of 2.41Hz, 2.53Hz and 2.62Hz from the full wind turbine model and with the natural frequency of 2.43Hz from the observation. The higher natural frequencies from the full wind turbine model correspond to the combined modes of the tower and blades identified by their mode shapes.

Table 4 Comparison of observed and predicted natural frequencies of the turbine

No	Natural frequencies (Hz)	Eigen frequencies (Hz)	
	Measurement	Full wind turbine model	Tower model
1	0.81	0.81	0.85
2	0.81	0.81	0.85
3	2.05	2.41	6.94
4	2.43	2.53	6.94
5	2.43	2.62	-
6	4.62	4.51	-
7	5.60	5.26	-
8	5.60	5.73	-
9	6.42	6.21	-
10	6.85	6.35	-

Table 5 Predicted natural frequencies for the blade model

No	Eigen frequencies (Hz)
1	2.58
2	6.19

Prediction of wind responses

The fluctuating velocities are generated by a method proposed by Iwatani (1982), and are used in the full dynamic simulation. Von Karman power spectrum model with phases of 0 and an exponent correlation with a decay factor of 8 were used for the fluctuating wind generation. The lateral and vertical turbulence intensity, I_v and I_w, were set as I_v=I_w=0.8I_u; and the integral length scale was assumed as L_v=L_w=0.5L_u. The wind profile for the alongwind component, U, is estimated by the power law corresponding to the terrain subcategory I as recommended by Architectural Institute of Japan (1996). Ten time series of the fluctuating wind velocity were generated and used to estimate fluctuating wind loads at 10 elevations of the wind turbine. The drag coefficient of 0.7 and 1.3 were used for the tower and the nacelle. The drag, lift and moment coefficients for each section of the blades were obtained by interpolating the existing data from GH Bladed (2001) for a blade with thickness to chord ratio of 12% and from James (2000) for a blade with thickness to chord ratio of 21%, as shown in Fig. 8.

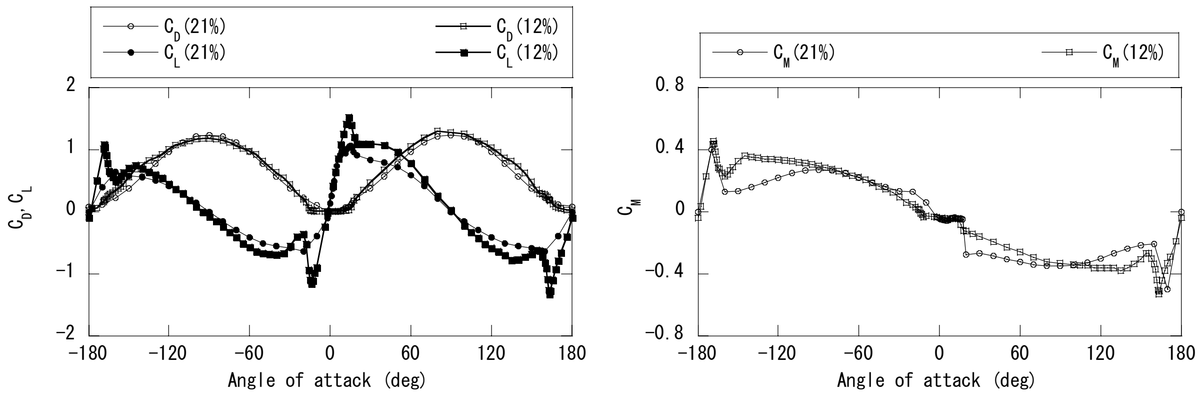

(a) Drag and Lift coefficients (b) Moment coefficient

Fig. 8 Variation of aerodynamic coefficients with the angle of attack

In addition, the structural damping ratios were assumed to be 1.0% and 0.6% in X and Y direction respectively. The simulation was carried out for 700 seconds by a time increment of 0.05 second and the first 100 seconds results were omitted for evaluation of the results in the 10 minutes and for comparison with the measurements.

Firstly, a 10-minute time series of the tower bending moments for the northerly wind (Jan. 21st, 2004 2:40~2:50) was simulated using the FEM code, CAsT. The response is calculated for a 10-minute mean wind speed of 20m/s and turbulence intensity of 11% at the hub height, corresponding to the measurement. Fig. 9 presents the comparison of observed and predicted time series of tower bending moments plotted in X-Y plane. Both of them draw an elliptical orbit with much the same amplitude. The fluctuations in the orbit are due to the stochastic turbulence field in conjunction with the rapid changes in the drag and lift coefficients of the blades with the angle of attack.

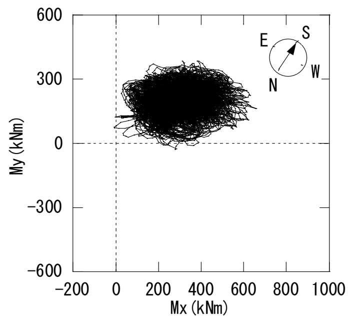

(a) Measurement

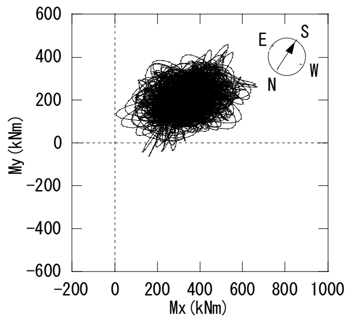

(b) Prediction

Fig. 9 Comparison of observed and predicted tower bending moments plotted in X-Y plane

In order to give a systematic evaluation, full dynamic simulations with the same model mentioned above were preformed using several mean wind speeds of 5, 10, 20, 25, 30 m/s for the northerly wind. The maximum, the mean and the standard deviation of the tower bending moment predicted by the full dynamic simulations are shown in Fig.13 and compared with the measurements. The predicted moments demonstrate a good agreement with the measurements.

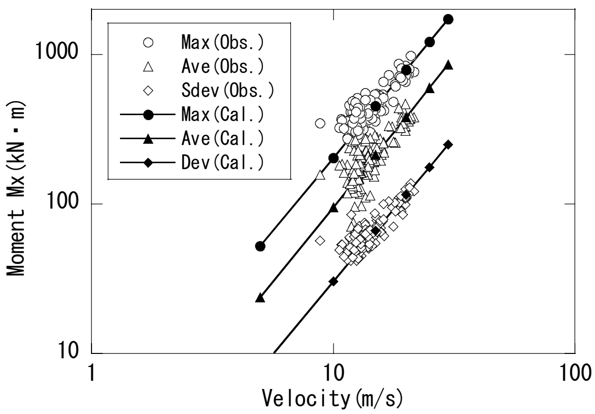

(a) X direction

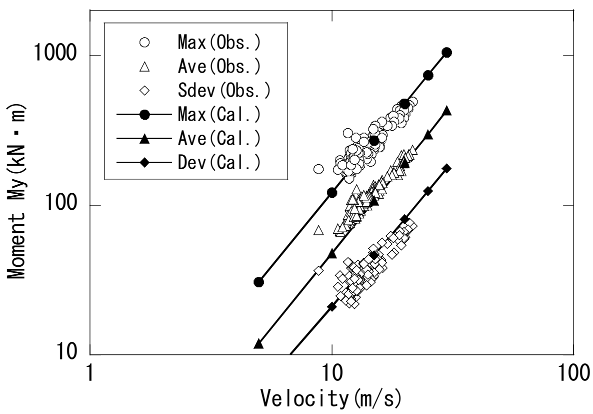

(b) Y direction

Fig. 10 Variation of tower bending moments with mean wind speeds in X and Y direction

CONCLUDING REMARKS

A field test on the NEG Micon stall regulated wind turbine with a rated power of 400 kW was carried out to investigate the structural parameters and response characteristics of the turbine. A FEM code was developed to predict the natural frequencies and wind responses of wind turbines, and the estimated wind loads were compared with the measurements. The finding and the conclusions are summarized as follows.

(1) The lower natural frequencies obtained from the observed accelerations, such as 0.81Hz, 2.43Hz, coincide with the first natural frequencies of the tower and blades, respectively. The damping ratios of the tower were around 1% in the fore-aft direction and 0.6% in the side-side direction.
(2) Using the full wind turbine model with beam elements, all observed natural frequencies of the wind turbine were reproduced. However, the tower model, in which blades, hub, nacelle were modeled by a concentrated mass at the top of tower, can not estimate the natural frequencies of the blade and shows slightly higher first natural frequency of the tower with 5% of error.
(3) The FEM code for the full dynamic simulation developed in this study was used to predict the maximum, the mean and the standard deviation of the tower bending moments and demonstrated a good agreement with the measurements.

ACKNOWLEGGEMENTS

Authors are deeply grateful to Dr. K.Shimada of Shimizu Co., Mr N. Kishi of Sun System Supply Co. and Dr. M. Shimizu of Central Research Institute of Electric Power Industry for their help and advices during the investigation.

REFERENCES

Architectural Institute of Japan (1996), *Recommendations for Loads on Buildings.*

GH Bladed (2001), Generic 2MW Offshore Turbine, GH Bladed Version3.51, *Garrad Hassan and Partners Limited*, 2001

Ishihara, T., Hibi, K., Kato, H., Ohtake, K., Matsui, M. (2002), A database of Annual Maximum Wind Speed and Corrections for Anemometers in Japan*, J. Wind Engineering JAWE*, Vol.92, 5-54 (in Japanese)

Ishihara, T., Yamaguchi, A., Takahara, K., Mekaru, T., Shinjo, F., Matsuura, S., Matsuura, S. (2005), An Analysis of Damaged Wind Turbines by Typhoon Maemi in 2003, *Proceedings of the Sixth Asia-Pacific Conference on Wind Engineering,* Korea.

Iwatani, Y. (1982), Simulation of multidimensional wind fluctuations having any arbitrary power spectra and cross spectra, *J. Wind Engineering*, JAWE, Vol.11, 5-17 (in Japanese)

James, R. S. (2000), Blind Code Runoff: Initial Yawdyn Model Description and Definitions, *Centre for Renewable Energy Systems Technology, Loughborough Univ.,* United Kingdom.

Riso National Laboratory (2001), *Guidelines for Design of Wind Turbines*, Wind Energy Department, Riso National Laboratory, Denmark.

Tamura, Y., Sasaki, A. and Tsukagoshi, H. (1991), Evaluation of damping ratio using the Random Decrement Technique, *Proceedings of '91 Annual Conf. of Architectural Institute of Japan*, Tohoku, 809-810 (in Japanese).